Dynamic Phasors-Based Modeling and Stability Analysis of Droop-Controlled Inverters for Microgrid Applications

Guo, Xiaoqiang; Lu, Zhigang; Wang, Baocheng; Sun, Xiaofeng; Wang, Lei ; Guerrero, Josep M.

Published in:
I E E E Transactions on Smart Grid

DOI (link to publication from Publisher):
10.1109/TSG.2014.2331280

Publication date:
2014

Document Version
Early version, also known as pre-print

This document is a preprint version of the paper:
X. Guo, Z. Lu, B. Wang, X. Sun, and J. M. Guerrero, "Dynamic Phasors Based Modeling and Stablity Analysis of Droop-Controlled Inverters for Microgrid Applications," IEEE Trans. Smart Grid, 2014, IEEE early access.

Dynamic Phasors Based Modeling and Stablity Analysis of Droop-Controlled Inverters for Microgrid Applications

Xiaoqiang Guo, *Member, IEEE,* Zhigang Lu, B. Wang, X. Sun, L. Wang and Josep M. Guerrero, *Senior Member, IEE*

***Abstract* –System modeling and stability analysis is one of the most important issues of inverter-dominated microgrids. It is useful to determine the system stability and optimize the control parameters. The complete small signal models for the inverter-dominated microgrids have been developed which are very accurate and could be found in literature. However, the modeling procedure will become very complex when the number of inverters in microgrid is large. One possible solution is to use the reduced-order small signal models for the inverter-dominated microgrids. Unfortunately, the reduced-order small signal models fail to predict the system instabilities. In order to solve the problem, a new modeling approach for inverter-dominated microgrids by using dynamic phasors is presented in this paper. Our findings indicate that the proposed dynamic phasor model is able to predict accurately the stability margins of the system, while the conventional reduced-order small signal model fails. In addition, the virtual *ω-E* frame power control method, which deals with the power coupling caused by the line impedance X/R characteristic, has also been chosen as an application example of the proposed modeling technique.**

***Index Terms*—microgrid, droop control, inverter, small signal mode, dynamic phasor, stability analysis,**

I. INTRODUCTION

The environmental concerns and electric utility deregulation promote the development of distributed generation (DG) in a rapid pace. When the levels of DG are comparable to the demand ones, allows forming microgrids [1-4]. A microgrid is defined as a cluster of DG units, such as wind turbines and/or photovoltaic systems, energy storage devices and local loads, which can operate in both grid-connected or islanded modes. Islanded microgrids operation is defined in the IEEE Std 1547.4-2011 and is the focus of this paper.

Manuscript received 2014. This work was supported by the National Natural Science Foundation of China under Awards 51307149 and Specialized Research Fund for the Doctoral Program of Higher Education (20131333120016).

X. Guo is with the Key Lab of Power Electronics for Energy Conservation and Motor Drive of Hebei Province, Department of Electrical Engineering, Yanshan University, Qinhuangdao 066004, China (e-mail: gxq@ysu.edu.cn).

J. M. Guerrero is with the Department of Energy Technology, Aalborg University, Aalborg DK-9220, Denmark (e-mail: joz@et.aau.dk).

In inverter-based islanded microgrids, the droop control is widely used to regulate the power flow according to the local information with no need of communication [5-18]. In hierarchical control terms, droop control constitutes primary control level, which defines frequency and voltage participation of each DG unit [5].

In the conventional droop control, the line impedance is considered to be mainly inductive. However, in low voltage grids the lines are mostly resistive, which may affect the way of controlling active and reactive power. Furthermore, the conventional droop control presents other drawbacks. In the past decades, many attempts have been made to improve the performance of the conventional droop control. A significant contribution is the virtual impedance concept [19]. For the accurate power sharing, the output impedance should be fixed as inductive, resistive or complex impedances. In [20], a virtual inductance is designed for the inductive output impedance even with high R/X ratio. On the other hand, the resistive output impedance is used [21], which ensures the system to be more damped and better power sharing. In [22], the virtual complex impedance is designed to minimize the circulating current for the efficient power sharing. Another interesting solution reported in [23] is the virtual frequency and voltage frame droop control. It can directly control the actual real and reactive power, but the frame transformation angle for each inverter should be the same, e.g. 45° .

On the other hand, the dynamic stability of inverter-based MicroGrid systems has been studied for many years. For that kind of applications, small-signal model is widely used since it is easy to predict the system response when changing parameters. Thus it is helpful to select control and system parameters. Furthermore, the microgrid configuration, operation modes, load locations, and the inverters connection, affect the small signal-modeling and stability.

The small signal model analysis has a long history in multi-machine systems. The typical contributions were made by Laughton in 1966 [24] and Uudrill in 1968 [25], which were mainly used for the system stability analysis. Recently, it was extended to the microgrid applications. The complete small signal models for the inverter-dominated microgrids have been developed in the literature [26-30], which are very

accurate to predict the system dynamic and stability. However, they become very computational and complex when the number of inverters in microgrid is large [31]. One possible solution is to use the reduced-order small signal models for the inverter-dominated microgrids. In [32], the authors assumed that the dynamics of the inner voltage/current controllers can be neglected, thus making the model much more simple. This assumption is acceptable since the inner voltage and current controls bandwidth are much higher than the outer droop control, due to the low pass filter used to average active and reactive powers. However, the reduced-order model neglects the dynamic of the power network circuit elements. This is acceptable for slow systems with high inertia, such as multi-machine power systems, but it can lead to questionable results for fast systems, such as power electronics based microgrids. On the other hand, dynamic phasor model is very simple and useful to predict the system dynamic and stability. In fact, it has been widely used in SSR [33], TCSC [34], UPFC [35], FACT [36], and so on. However, its use for the inverter-dominated microgrid has not received much attention.

This paper presents a dynamic phasor model (DPM) for inverter-dominated autonomous microgrids. This model takes into account the dynamic of the power network circuit elements. The comparison between the small signal model by using the conventional modeling method and the DPM is performed by means of simulation results, showing that DPM presents higher precision when predicting the transient response and ability to determine the stability limits.

Moreover, a case study of the virtual ω–E frame power control method is also presented here. This virtual frame was proposed in order to deal with the active and reactive power coupling emphasized by the line impedance characteristic [23]. For this case and the conventional droop one, the DPM is created, and the root locus analysis reveals that this method can greatly improve the system stability. This paper is organized as follows. The system configuration and control scheme is shown in Section II. The small-signal closed-loop model is developed in Section III. The DPM is proposed in Section IV. The sensitivity analysis and modeling for the conventional droop control method is verified in Section V. Section VI presents the DPM of the virtual ω–E frame power control. Conclusions are given in Section VII.

II. System Configuration and Control Scheme

Fig. 1 illustrates the power stage of an inverter-based microgrid [23], which includes energy sources with optional energy storage and dc/ac inverters. The inverters can provide for flexible functionalities such as voltage/frequency control and power quality improvement. The inverter output may either feed the local loads independently in autonomous mode or in conjunction with the electric utility by static switch (STS) in grid connected mode. This paper will focus on the autonomous mode.

In Fig. 1, E_n (n=1, 2) and V are the amplitudes of the inverter output voltage and the ac bus voltage respectively, δ_n is the power angle difference, Z_n and θ_n are the magnitude and the phase of the line impedance respectively.

The inverter output active and reactive power can be expressed according to Fig.1 as follows:

$$P = \frac{3}{R^2 + X^2}(RE^2 - REV\cos\delta + XEV\sin\delta) \tag{1}$$

$$Q = \frac{3}{R^2 + X^2}(XE^2 - XEV\cos\delta - REV\sin\delta) \tag{2}$$

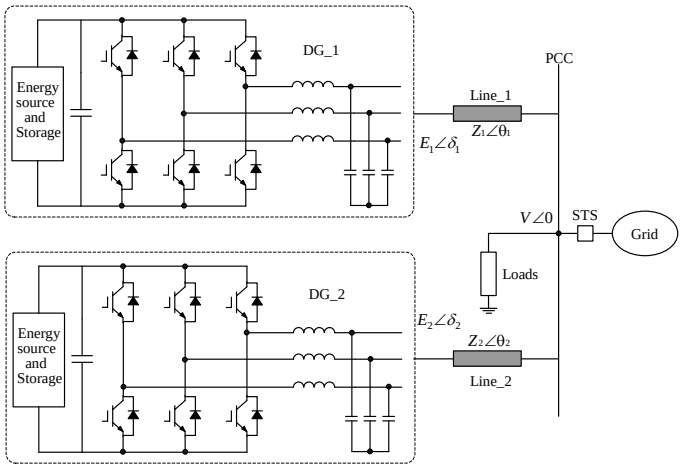

Fig.1 Schematic diagram of an inverter-based microgrid.

where R and X are the resistive and inductive output impedance components, and δ the power angle.

In order to clarify the basic principle of the power droop control, the sensitivity analysis is carried out as follows.

$$\frac{\partial P}{\partial \delta} = \frac{3(REV\sin\delta + XEV\cos\delta)}{R^2 + X^2} \tag{3}$$

$$\frac{\partial P}{\partial E} = \frac{3(2RE - RV\cos\delta + XV\sin\delta)}{R^2 + X^2} \tag{4}$$

$$\frac{\partial Q}{\partial \delta} = \frac{3(XEV\sin\delta - REV\cos\delta)}{R^2 + X^2} \tag{5}$$

$$\frac{\partial Q}{\partial E} = \frac{3(2XE - XV\cos\delta - RV\sin\delta)}{R^2 + X^2}. \tag{6}$$

Note that the power angle δ is relatively small in practice, so that we can approximate $\sin\delta \approx 0$ and $\cos\delta \approx 1$. Thus, equations (3) to (6) can be simplified as following:

$$\frac{\partial P}{\partial \delta} = \frac{3XEV}{R^2 + X^2} \tag{7}$$

$$\frac{\partial P}{\partial E} = \frac{3(2RE - RV)}{R^2 + X^2} \tag{8}$$

$$\frac{\partial Q}{\partial \delta} = \frac{-3REV}{R^2 + X^2} \tag{9}$$

$$\frac{\partial Q}{\partial E} = \frac{3(2XE - XV)}{R^2 + X^2} \tag{10}$$

When the line impedance is mainly inductive, that is $R \approx 0$, equations (7) to (10) can be rewritten as follows: $\frac{\partial P}{\partial \delta} = \frac{3EV}{X}$, $\frac{\partial P}{\partial E} \approx 0$, $\frac{\partial Q}{\partial \delta} \approx 0$, and $\frac{\partial Q}{\partial E} = \frac{6E - 3V}{X}$. Therefore, it can be observed that the active power P is more dependent on the power angle, and hence frequency, variations, while the reactive power Q is more sensitive to the output voltage magnitude variation. That is why *P-f* and *Q-V* droop control schemes are widely used in power systems, which can be expressed as follows:

$$\omega = \omega^* - k_p(P - P^*) \tag{11}$$

$$E = E^* - k_q(Q - Q^*) \tag{12}$$

where k_p and k_q the frequency and voltage droop coefficients, and P^* and Q^* are the power references.

It should be noted that there are three control levels for the microgrid, as specified in [5], and this paper mainly concerns the droop control level (Level 1).

III. Small Signal Modeling Review

In this Section, a general procedure will be carried out in order to obtain the small signal model of the system described in Fig. 1.

For small disturbances around the equilibrium point (δ_e, E_e, V_e) of equation (1), (2), (11) and (12), the following linearized equations can be obtained, as reported by Coelho in [37-38].

$$\Delta\omega = \Delta\omega^* - k_p\Delta P + k_p\Delta P^* \tag{13}$$

$$\Delta E = \Delta E^* - k_q\Delta Q + k_q\Delta Q^* \tag{14}$$

$$\Delta P = k_{pe}\Delta E + k_{pd}\Delta\delta \tag{15}$$

$$\Delta Q = k_{qe}\Delta E + k_{qd}\Delta\delta \tag{16}$$

where

$$k_{pe} = \frac{3RE}{R^2 + X^2} \tag{17}$$

$$k_{pd} = \frac{3XE^2}{R^2 + X^2} \tag{18}$$

$$k_{qe} = \frac{3XE}{R^2 + X^2} \tag{19}$$

$$k_{qd} = \frac{-3RE^2}{R^2 + X^2} \tag{20}$$

In order to measure the inverter output active and reactive power, a low pass filter is often used. Thus, the active and reactive powers are obtained by averaging over a grid line frequency by using a low pass filter that can be represented by the following first order expressions:

$$\Delta p = \frac{\omega_f}{s + \omega_f}\Delta P \tag{21}$$

$$\Delta q = \frac{\omega_f}{s + \omega_f}\Delta Q \tag{22}$$

being Δp and Δq the average values of ΔP and ΔQ.

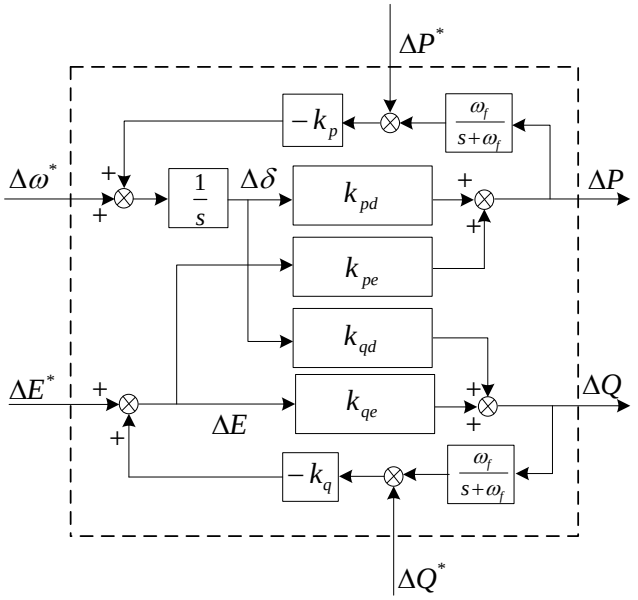

Fig. 2. Small signal close-loop model.

From the aforementioned analysis, it is possible to obtain the small signal closed-loop model, as shown in Fig. 2. The references ω^*, E^*, P^*, and Q^* are considered to be constant here, so their deviation term in (13) and (14) can be neglected.

Due to the low pass filter, the inner voltage and current control bandwidth are much higher than the outer power loop. So that, it can be assumed that the dynamics of the inner loops can be neglected. Thus, the inverter output voltage is considered to be directly governed by the references generated by the droop control strategy.

Considering the above assumption, by combining equations (13) to (22), we can get the frequency and voltage dynamics expressed as following:

$$\Delta\omega = -\frac{k_p\omega_f}{s + \omega_f}(k_{pe}\Delta E + k_{pd}\Delta\delta) \tag{23}$$

$$\Delta E = -\frac{k_q\omega_f}{s + \omega_f}(k_{qe}\Delta E + k_{qd}\Delta\delta) \tag{24}$$

The phase angle is the integral of the frequency, so that it can be expressed as:

$$\Delta\omega = s\Delta\delta \tag{25}$$

By combining equations (23) to (25), the characteristic equation of the close loop system with the conventional droop is obtained as:

$$s^3 + as^2 + bs + c = 0 \tag{26}$$

where

$$a = (2 + k_q k_{qe})\omega_f$$

$$b = (k_p k_{pd} + k_q k_{qe}\omega_f + \omega_f)\omega_f$$

$$c = (k_{pd} + k_q k_{pd} k_{qe} - k_q k_{pe} k_{qd})k_p\omega_f^2$$

The coefficients of the characteristic equation (26) determine the system transient response, roots and therefore the closed loop stability.

It should be noted that in this model, which original proposed by Coelho in 1999, $X=\omega L$ and ω is considered constant, not dynamic, which is the inherent limitation of this model. In the next section, we will try to overcome this limitation by using dynamic phasors based model.

IV. Dynamic Phasor Modeling

The small signal model described in Section III neglects the dynamic of the power network circuit elements. This model is acceptable for high inertial systems like [25], but it can lead to questionable results for power electronics inverter based system. To deal with this problem, this Section proposes a dynamic phasors based model.

The concept of dynamic phasor has been developed to model the power converters for a long time [39-40]. But its application to microgrid model has not well explored. In this Section, the dynamic phasor concept is used for modeling purposes of the inverter-dominated autonomous microgrid as shown in Fig.1. This modeling will be called hereinafter dynamic phasor model (DPM).

The generalized averaging to obtain the DPM is based on the property that a possible complex time domain waveform $x(\tau)$ can be represented inside the interval $\tau \in (t-T, t]$ by the following Fourier series [40]:

$$x(\tau) = \sum_{k=-\infty}^{\infty} X_k(t) e^{jk\omega_s \tau} \tag{27}$$

being $\omega_s = 2\pi/T$ and $X_k(t)$ are the complex Fourier coefficients also named *phasors*. The dynamic or time-varying k^{th} phasor at time t, $X_k(t)$, can be expressed in its integral form defined inside the time interval by means of [39]:

$$X_k(t) = \frac{1}{T}\int_{t-T}^{t} x(\tau) e^{-jk\omega_s \tau} d\tau = \langle x \rangle_k (t) \tag{28}$$

being $\langle x \rangle_k(t)$ the average k-th phase over the period T.

An important property of the phasors is the derivative with respect to the time of the k^{th} dynamic phasor X_k, which can be expressed as follows:

$$dX_k(t)/dt = \langle dx/dt \rangle_k (t) - jk\omega_s X_k(t) \tag{29}$$

Consequently, for instance, the relationship between an inductor voltage v_L and its current i_L can be expressed by:

$$v_L = L(di_L/dt) + j\omega L i_L \tag{30}$$

being L the inductance value and ω the operation frequency. Notice that in conventional circuit theory, the second term on the right hand of (30), $j\omega L i_L$, does not exist.

At this point, we have a dynamic but linear model. From (30), we can rewrite the inverter output active and reactive powers from Fig.1, yielding (see appendix for details):

$$P = 3\frac{Ls+R}{(Ls+R)^2+(\omega L)^2}(E^2 - EV\cos\delta) + 3\frac{\omega L}{(Ls+R)^2+(\omega L)^2} EV\sin\delta \tag{31}$$

$$Q = 3\frac{\omega L}{(Ls+R)^2+(\omega L)^2}(E^2 - EV\cos\delta) - 3\frac{Ls+R}{(Ls+R)^2+(\omega L)^2} EV\sin\delta \tag{32}$$

For small disturbances around the equilibrium point (δ_e, E_e, V_e), the linearized equations can be obtained.

$$\Delta P = k_{pe}^{'}\Delta E + k_{pd}^{'}\Delta\delta \tag{33}$$

$$\Delta Q = k_{qe}^{'}\Delta E + k_{qd}^{'}\Delta\delta \tag{34}$$

where

$$k_{pe}^{'} = \frac{3(Ls+R)E}{(Ls+R)^2+(\omega L)^2}$$

$$k_{pd}^{'} = \frac{3\omega L E^2}{(Ls+R)^2+(\omega L)^2}$$

$$k_{qe}^{'} = \frac{3\omega L E}{(Ls+R)^2+(\omega L)^2}$$

$$k_{qd}^{'} = \frac{-3(Ls+R)E^2}{(Ls+R)^2+(\omega L)^2}$$

From the abovementioned analysis, the DPM characteristic equation can be obtained as

$$a^{'}s^5 + b^{'}s^4 + c^{'}s^3 + d^{'}s^2 + e^{'}s + f^{'} = 0 \tag{35}$$

Where

$$a^{'} = L^2 \qquad b^{'} = 2RL + 2\omega_f L^2$$

$$c^{'} = R^2 + \omega^2 L^2 + 4RL\omega_f + L^2\omega_f^2$$

$$d^{'} = 2R^2\omega_f + 2\omega_f\omega^2 L^2 + 2RL\omega_f^2 + 3\omega LEk_q\omega_f$$

$$e^{'} = R^2\omega_f^2 + \omega^2 L^2\omega_f^2 + 3\omega LEk_q\omega_f^2 + 3\omega LE^2 k_p\omega_f$$

$$f^{'} = 3\omega LE^2 k_p\omega_f^2 + 9E^3 k_p k_q \omega_f^2$$

The coefficients from (35) determine the roots and therefore the closed loop stability of the DPM. From a computational point of view, it can be observed that the modeling procedure is simper than the conventional one [31] to predict the system instabilities. It should be noted that in this model, the dynamics of network elements (See (30)) are now taking into account, which is in contrast with the model reported in [37]. The Following will provide a comparison and discussion about the complete model [27], reduce-order model [37] and the proposed model.

V. Sensitivity Analysis and Model verification

Section III presented the conventional reduce-order small-signal modeling of a droop controlled inverter, while Section IV introduced the proposed DPM approach. In this Section, a comparison about the complete model [27], reduce-order model [37] and the proposed model is carried out. Considering the complete model in [27] has been verified to be accurate enough, it is used as a benchmark here to compare with the other models. The detailed modeling procedure has been reported in [27], and not duplicated here any more. A sensitivity analysis is conducted in order to compare three models. Simulation studies start from t=0. It is a step change from 0 to some level of power. The similar simulation procedure can be found in [17], [22]. Simulation results will be performed by using the system shown in Fig. 1, in order to show which model is more accurate compared with the complete model in [27].

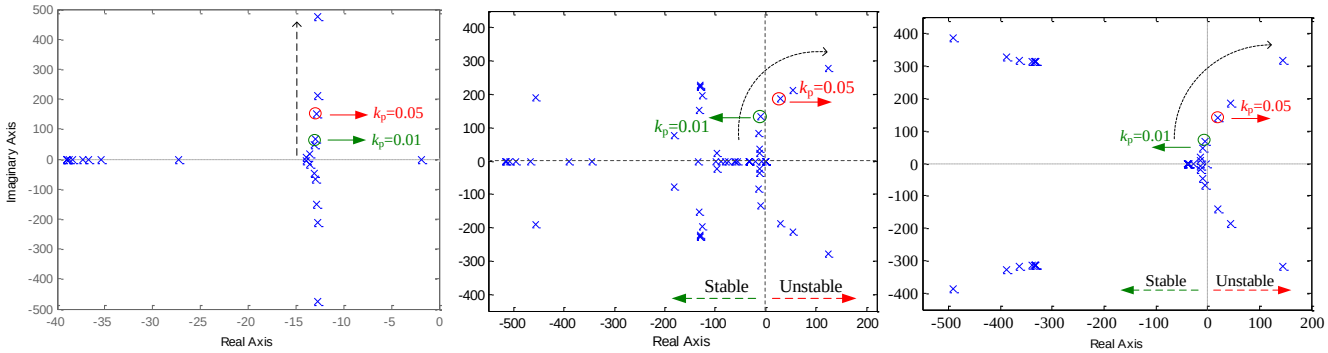

(a) Small signal model [37] (b) Complete model [27] (c) Proposed DPM

Fig. 3. Dominant eigenvalues comparison for k_p variations.

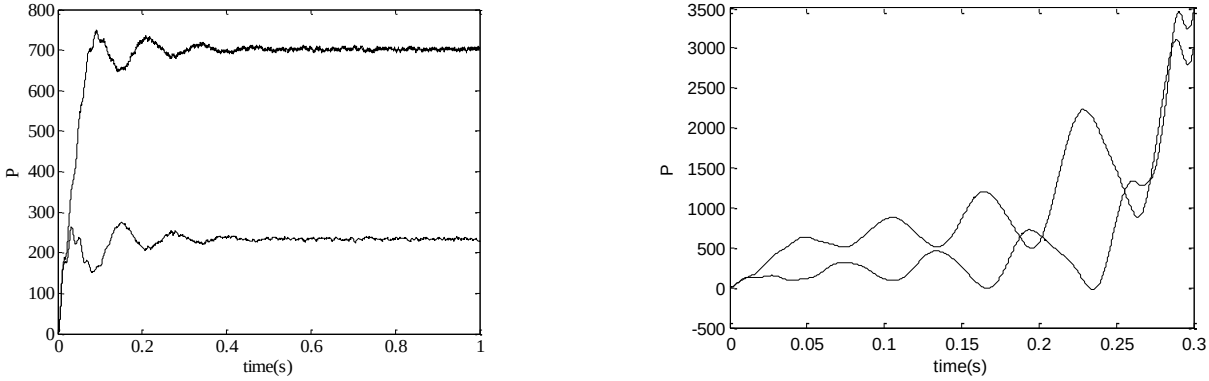

(a) k_p = 0.01 (stable) (b) k_p = 0.05 (unstable)

Fig, 4. Inverters output active power for k_p variations.

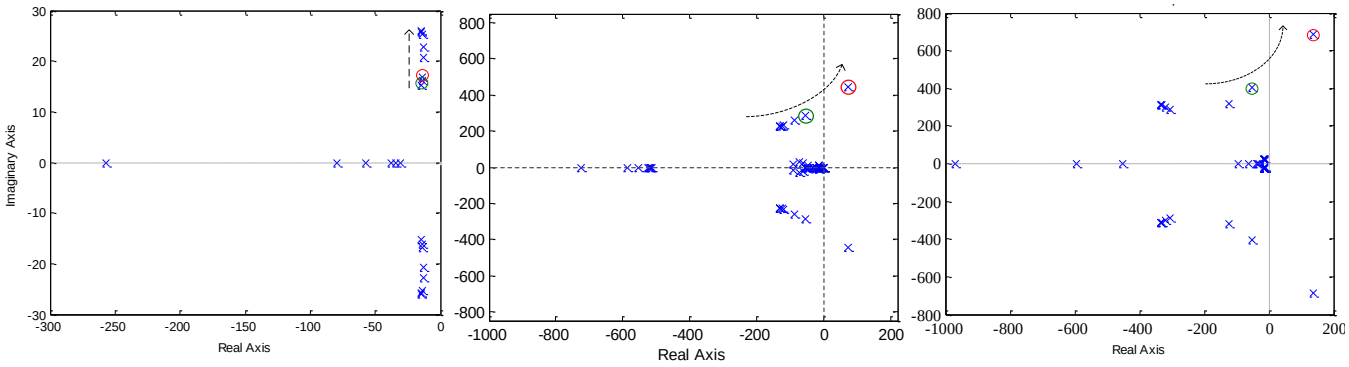

(a) Small signal model [37] (b) Complete model [27] (c) Proposed DPM

Fig. 5. Dominant eigenvalues comparison for k_q variations.

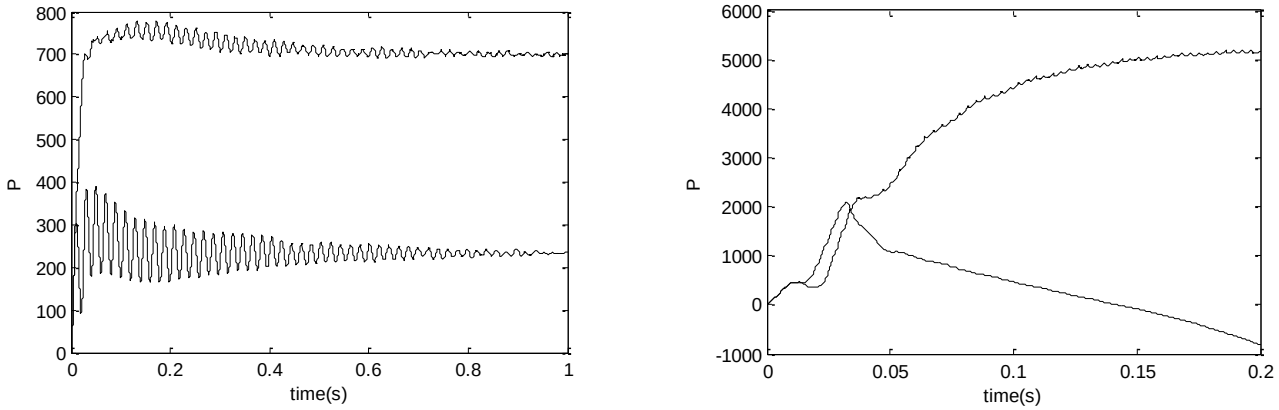

(a) k_q = 0.1 (stable) (b) k_q = 0.5 (unstable)

Fig. 6. Inverters output active power for k_q variations.

TABLE I. SYSTEM PARAMETERS

Parameter	*Value*
DC link voltage	250 V
filter inductance	3 mH
filter capacitance	9.9 μF
line impedance	1+j 1 Ω
output voltage	100 V/50Hz
low pass filter frequency	one decade below 50Hz

The system parameters used in this analysis are shown in Table I. It should be noted that a low pass filter is used to avoid the interaction between the power control loop and voltage/current control loop. The cutoff frequency of the filter is generally one decade below 50Hz, as reported in [8]

In order to investigate the sensitivity analysis and model verification, we change the droop coefficients by setting a series of number from 0.0001 to 0.5 with the MATLAB function. In this way, the coefficients can be automatically generated from 0.0001 to 0.5. For the analysis, it has been considered that the nominal power of inverter #1 is two times bigger than that of inverter #2. The active power droop gain of inverter #1, k_p, has been changed from 0.0001 to 0.5, and the reactive power droop gain of inverter #1, k_q, is also changed from 0.0001 to 0.5. Consequently, the droop coefficients values of inverter #2 are double than those of inverter #1, accordingly.

The dominant eigenvalues comparison of three models when k_p increasing is shown in Fig.3. Note that the complete model in [27] has been verified to be accurate enough. It is used as a benchmark here to compare with the other models. Fig. 3(a) shows the dominant eigenvalues of the complete model. In agreement with the conclusion of [27], the system tends to be unstable when the real power droop gain k_p increases. On the other hand, as shown in Fig. 3(b) and Fig. 3(c), the reduced-order model shows that all the poles are in the left half-plane, while the DPM shows that some of the poles move to right half plane, which will make the system unstable. From Fig.3, it can be observed that the reduced-order model is quite different from the complete model. The proposed DPM is slight different from the complete model due to neglecting the high bandwidth voltage/current loop, but the dominant eigenvalues movement trend is very similar, which is useful to determine the system stability. Simulation results by using the parameters of the green circle (k_p=0.01) and the red circle (k_p=0.05) in Fig. 3, are shown in Fig. 4. It can be seen that the system is stable when k_p is 0.01, but unstable when k_p is 0.05. The simulation results are consistent with the complete model and DPM, showing that the stability margins were well predicted by this model.

Fig. 5 shows the dominant eigenvalues comparison of three models when increasing k_q. Fig. 5(a) shows the dominant eigenvalues of the complete model. In agreement with the conclusion of [27], the system tends to be unstable when the reactive power droop gain k_q increases. On the other hand, as shown in Fig. 5(b) and Fig. 5(c), the reduce-order model shows that all the poles are in the left half-plane, while the DPM shows that some poles move toward the right half plane and may cause the system unstable. Simulation results using the parameters of the green circle (k_q=0.1) and the red circle (k_q=0.5) in Fig. 5, are shown in Fig. 6. It can be seen that the system is stable when k_q is 0.1, but unstable when k_q is 0.5. Here also the simulation results are consistent with the DPM, showing the clear limitation of the reduced-order modeling.

Through the simulation results, we can draw the conclusion that the dynamic model is more precise than the reduced-order small signal model, which is not able to predict that stability limit.

VI. APPLICATION EXAMPLE: DYNAMIC PHASOR MODEL OF POWER DECOUPLING DROOP METHOD

As discussed earlier, the proposed model method can be successfully used for the stability analysis of the conventional droop method. However, the conventional droop method is only effective on condition that the line impedance is mainly inductive. Under the resistive-inductive impedance conditions, the active and reactive power coupling will be serious to affect the system stability. In order to solve the problem, many improved droop control methods have been proposed in order to deal with the power coupling problem. Reader might wonder whether the proposed modeling method in this paper can be extended to the improved droop method.

In order to answer this question, this section will present an illustrative example of the application of the DPM approach for the other droop method. Taking the virtual ω–E frame droop control [23] for example. By using the virtual ω–E frame power control, the inverter output frequency ω and the inverter output voltage E are controlled by the following droop characteristics:

$$\omega' = \omega'^{*} - k_p(P - P^{*}) \tag{36}$$

$$E' = E'^{*} - k_q(Q - Q^{*}) \tag{37}$$

where the following virtual frame is defined:

$$\begin{bmatrix} \omega' \\ E' \end{bmatrix} = \begin{bmatrix} \cos\varphi & \sin\varphi \\ -\sin\varphi & \cos\varphi \end{bmatrix} \begin{bmatrix} \omega \\ E \end{bmatrix}, \varphi = 90^{\circ} - \theta \tag{38}$$

For small disturbances around the equilibrium point (δ_e, E_e, V_e), the linearized equations following can be obtained:

$$\Delta\omega\cos\varphi + \Delta E\sin\varphi = -k_p\Delta P \tag{39}$$

$$\Delta E\cos\varphi - \Delta\omega\sin\varphi = -k_q\Delta Q \tag{40}$$

From the abovementioned analysis, the DPM characteristic equation now takes the form:

$$a''s^5 + b''s^4 + c''s^3 + d''s^2 + e''s + f'' = 0 \tag{41}$$

where

$$a'' = L^2$$

$$b'' = 2RL + 2\omega_f L^2$$

$$c'' = R^2 + \omega^2 L^2 + 4RL\omega_f + L^2\omega_f^2 + 3k_p\omega_f LE\sin\varphi$$

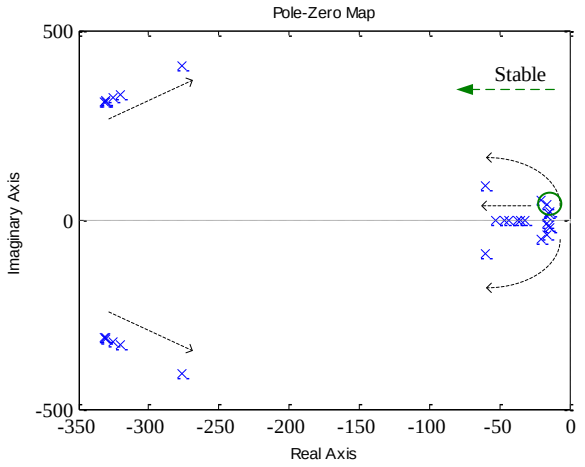

Fig. 7. Root locus of the DPM with virtual ω-E frame power control for k_p variations.

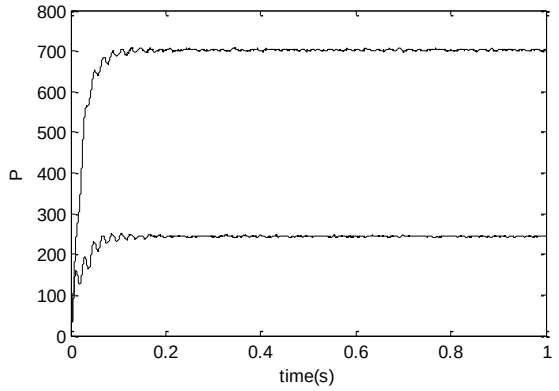

Fig, 8. The inverters output active power with the virtual ω–E frame power control when k_p is 0.05 (stable)

$$d^{"} = 2R^2\omega_f + 2\omega_f\omega^2L^2 + 2RL\omega_f^2 + 3k_q\omega_f E^2 L\sin\varphi + 3k_q\omega_f\omega LE\cos\varphi + 3k_p\omega_f^2 LE\sin\varphi + 3k_p\omega_f RE\sin\varphi$$

$$e^{"} = R^2\omega_f^2 + \omega^2L^2\omega_f^2 + 3k_q\omega_f^2E^2L\sin\varphi + 3k_q\omega_f E^2R\sin\varphi + 3k_q\omega_f^2\omega LE\cos\varphi + 3k_p\omega_f^2 RE\sin\varphi + 3k_p\omega_f\omega LE^2\cos\varphi$$

$$f^{"} = 3k_q\omega_f^2E^2R\sin\varphi + 3k_p\omega_f^2\omega LE^2\cos\varphi + 9k_pk_q\omega_f^2E^3$$

It is our worth to note that when the line impedance angle is 90 degrees, then φ will be 0 degrees, and in this situation the characteristic equation in (41) is exactly the same as the one shown in (35).

Fig. 7 shows the root locus of the DPM of the closed loop system when using the virtual ω–E frame power control for k_p variations. By comparing Fig. 7 with Fig. 3(b), it can be seen that the dynamic response is much faster than the conventional droop control. Notice that for this control approach all the poles are at the left half-plane, so that the system is stable. Simulation result when using the virtual ω–E frame power control shown in Fig. 8, k_p is 0.05 here. It can be observed that by using the power decoupling droop method, the system stability is greatly improved.

VII. Discussion and Conclusion

In this paper, the modeling and stability analysis of the droop-controlled inverter-dominated autonomous microgrid is discussed. The conventional reduced-order small-signal model and the proposed dynamic phasor model are obtained and compared. The reduced-order small-signal model shows that the system keeps stable even when using large droop gains. However, the large signal simulation results show that this is not realistic. Thus, the conventional reduced-order small signal model is not precise enough to study the dynamics and stability of droop-controlled inverter-dominated autonomous microgrids.

To deal with the model precision problem, a dynamic phasor based modeling approach is used. This method takes the dynamic of the power network circuit elements into account. Simulation results show that this model can be used to accurately predict the system stability limits. Hence, we can obtain the droop gains that make the system stable, but the reduced-order small-signal model fails when trying to obtain those. As a result, we can conclude that the proposed dynamic phasor model is more precise and can be used to design the control and power stage parameters of the real system.

It should be noted that, from the compete model accuracy viewpoint, the proposed dynamic phasor model might not be as accurate as the complete model in [27], mainly due to neglecting the high-bandwidth voltage/current loop. However, the proposed dynamic phasor model can predict the dominant eigenvalues movement trend, which is very similar to the compete model. And it is very useful to predict the system stability limits, which is mainly determined by the low bandwidth dominant eigenvalues, as reported in [27]. Table II provides a brief comparison of three models.

Table II. Comparion of Three Models

Model name	Accuracy	Modeling procedure
Reduced-order model [37]	Low	Easy
Complete-order model [27]	High	Complex
Proposed model	Fair	Easy

Finally, the proposed modeling approach can be extended to other control techniques. As an illustrative example, in order to deal with the power coupling caused by the line impedance, a virtual ω–E frame power control method is analyzed. Thus, the dynamic phasor model was obtained, and the root locus shown that this method can greatly improve the system stability, predicting once again the stability performance of the closed loops system.

It should be noted that our proposed model, as well as all the existing models, will be complex if large microgrid with dynamically different sources (renewable sources/storage/ machine based sources) integration is considered. It needs further investigation, and will be the subject of our future research.

APPENDIX

From Fig.1 and equation (30), the apparent power can be expressed as:

$$S = P(t) + jQ(t) = 3\dot{E}\dot{I}^* \tag{A1}$$

where $\dot{I} = \dfrac{\dot{E} - \dot{V}}{Ls + R + j\omega L}$

With mathematic manipulation,

$$\begin{aligned} P(t) + jQ(t) &= \frac{3\dot{E}(\dot{E}^* - \dot{V}^*)}{Ls + R - j\omega L} \\ &= \frac{3\dot{E}(\dot{E}^* - \dot{V}^*)(Ls + R + j\omega L)}{(Ls + R)^2 + (\omega L)^2} \\ &= \frac{[3E^2 - 3V(E\cos\delta + jE\sin\delta)](Ls + R + j\omega L)}{(Ls + R)^2 + (\omega L)^2} \end{aligned} \tag{A2}$$

Expand the above equation, and then we can obtain (A3) and (A4) as follows.

$$P = 3\frac{Ls + R}{(Ls + R)^2 + (\omega L)^2}(E^2 - EV\cos\delta) + 3\frac{\omega L}{(Ls + R)^2 + (\omega L)^2}EV\sin\delta \tag{A3}$$

$$Q = 3\frac{\omega L}{(Ls + R)^2 + (\omega L)^2}(E^2 - EV\cos\delta) - 3\frac{Ls + R}{(Ls + R)^2 + (\omega L)^2}EV\sin\delta \tag{A4}$$

REFERENCES

[1] X. Liu, P. Wang, and P. C. Loh, "A hybrid ac/dc microgrid and its coordination control," *IEEE Trans. Smart Grid*, vol. 2, no. 2, pp. 278–286, Jun. 2011.

[2] A. Radwan and Y. Mohamed, "Linear active stabilization of converter dominated dc microgrids," *IEEE Trans. Smart Grid*, vol. 3, no. 1, pp. 203–216, Mar. 2012.

[3] A. Radwan and Y. Mohamed, "Modeling, analysis, and stabilization of converter-fed ac microgrids with high penetration of converter-interfaced loads," *IEEE Trans. Smart Grids*, vol. 3, no. 3, pp. 1213–1225, Sep. 2012.

[4] A. Radwan and Y. Mohamed, "Assessment and mitigation of interaction dynamics in hybrid ac/dc distribution generation systems," *IEEE Trans. Smart Grid*, vol. 3, no. 3, pp. 1382–1393, Sep. 2012.

[5] J. M. Guerrero, J. C. Vasquez, J. Matas, L. G. de Vicuna, and M. Castilla, "Hierarchical control of droop-controlled AC and DC microgrids—A general approach toward standardization," *IEEE Trans. Ind. Electron.*, vol. 58, no. 1, pp. 158–172, Jan. 2011.

[6] Y. W. Li, D. M. Vilathgamuwa, and P. C. Loh, "Design, analysis, and real-time testing of a controller for multibus microgrid system," *IEEE Trans. Power Electron.*, vol. 19, no. 5, pp. 1195–1204, Sep. 2004.

[7] K. D. Brabandere, B. Bolsens, J. V. D. keybus, A. Woyte, and J. Driesen, "A voltage and frequency droop control method for parallel inverters," *IEEE Trans. Power Electron.*, vol. 22, pp. 1107–1115, Jul. 2007.

[8] J. Kim, J. M. Guerrero, P. Rodriguez, R. Theodorescu, and K. Nam, "Mode adaptive droop control with virtual output impedances for inverter-based flexible AC microgrid," *IEEE Trans. Power Electron.*, vol. 26, no. 3, pp. 689–701, Mar. 2011.

[9] J. M. Guerrero, J. C. Vásquez, J. Matas, M. Castilla, and L. G. de Vicuña, "Control strategy for flexible microgrids based on parallel line-interactive UPS systems," *IEEE Trans. Ind. Electron.*, vol. 56, no. 3, pp. 726–735, Aug. 2009.

[10] T. L. Vandoorn, B. Renders, L. Degroote, B. Meersman, and L. Vandevelde, "Active load control in islanded microgrids based on the grid voltage," *IEEE Trans. Smart Grid*, vol. 2, no. 1, pp. 139–151, Mar. 2011.

[11] M. Savaghebi, A. Jalilian, J. C. Vasquez, and J. M. Guerrero, "Secondary control scheme for voltage unbalance compensation in an islanded droop-controlled microgrid," *IEEE Trans. Smart Grid*, vol. 3, no. 2, pp. 797–807, Jun. 2012.

[12] C. Sao and P. Lehn, "Control and power management of converter fed microgrids," IEEE Trans. Power Syst., vol. 23, no. 3, Aug. 2008.

[13] Y.A.-R. I. Mohamed and A. Radwan, "Hierarchical control system for robust micro-grid operation and seamless mode-transfer in active distribution systems," *IEEE Trans. Smart Grid*, vol. 2, no. 2, pp. 352–362, Jun. 2011.

[14] R. Majumder, B. Chaudhuri, A. Ghosh, R. Majumder, G. Ledwich, and F. Zare, "Improvement of stability and load sharing in an autonomous microgrid using supplementary droop control loop," *IEEE Trans. Power Sys.*, vol. 25, pp. 796–808, Jul. 2010.

[15] P. C. Loh and F. Blaabjerg, "Autonomous control of distributed storages in microgrids," in *Proc. IEEE Int. Conf. Power Electron. and ECCE Asia*, May/Jun. 2011, pp. 536–542.

[16] P. C. Loh, D. Li, Y. K. Chai, and F. Blaabjerg, "Autonomous operation of hybrid AC–DC microgrids with progressive energy flow tuning," in *Proc. IEEE-APEC'12*, Feb. 2012, pp. 1056–1060.

[17] J. He and Y. W. Li, "An enhanced microgrid load demand sharing strategy," *IEEE Trans. Power Electron*., vol. 27, no. 9, pp. 3984-3995, Jan. 2013.

[18] Q. Zhang, "Robust droop controller for accurate proportional load sharing among inverters operated in parallel," *IEEE Trans. Ind. Electron*., vol. 60, no. 4, pp.1281-1290, Apr. 2013.

[19] J. M. Guerrero, J. Matas, L. G. Vicuna, M. Castilla, and J. Miret, "Decentralized control for parallel operation of distributed generation inverters using resistive output impedance," *IEEE Trans. Ind. Electron*., vol. 54, pp. 994–1004, Apr. 2007.

[20] Y. W. Li and C. N. Kao, "An accurate power control strategy for power electronics-interfaced distributed generation units operating in a low voltage multibus microgrid," *IEEE Trans. Power Electron.*, vol. 24, pp. 2977–2988, Dec. 2009.

[21] J. M. Guerrero, L. G. Vicuna, J. Matas, M. Castilla, and J. Miret, "Output impedance design of parallel-connected UPS inverters with wireless load-sharing control," *IEEE Trans. Ind. Electron.*, vol. 52, pp. 1126–1135, Aug. 2005.

[22] W. Yao, M. Chen, J. Matas, J. Guerrero, and Z. Qian, "Design and analysis of the droop control method for parallel inverters considering the impact of the complex impedance on the power sharing," *IEEE Trans. Ind. Electron.*, vol. 58, no. 2, pp. 576 –588, Feb. 2011.

[23] Y. Li and Y. W. Li, "Power management of inverter interfaced autonomous microgrid based on virtual frequency-voltage frame," *IEEE Trans. Smart Grid.*, vol. 2, no. 1, pp. 30–40, Mar. 2011.

[24] M. A. Laughton, "Matrix analysis of dynamic stability in synchronous multimachine systems," *Proc. IEE*, vol. 113, no.2, pp. 325-336, Feb. 1966.

[25] J. M. Uudrill, "Dynamic Stability Calculations for an Arbitrary Number of Interconnected Synchronous Machines," *IEEE Trans. on Power Apparatus and Systems*, vol.PAS-87, no.3, pp. 835-844, March 1968.

[26] Katiraei, F.; Iravani, M.R.; Lehn, P.W., "Small-signal dynamic model of a micro-grid including conventional and electronically interfaced distributed resources," *Generation, Transmission & Distribution, IET* , vol.1, no.3, pp.369-378, May 2007

[27] N. Pogaku, M. Prodanovic, and T. C. Green, "Modeling, analysis and testing of autonomous operation of an inverter-based microgrid," *IEEE Trans. Power Electron.*, vol. 22, no. 2, pp. 613–625, Mar. 2007.

[28] R. Majumder, B. Chaudhuri, A. Ghosh, "Improvement of stability and load sharing in an autonomous microgrid using supplementary droop control loop," *IEEE Trans. Power Sys*., vol. 25, no.2, pp.796-808, May 2010.

[29] R. Majumder, "Some aspects of stability in microgrids," *IEEE Trans. Power Syst.*, vol. 28, no. 3, pp. 3243-3252, Aug. 2013.

[30] E. Barklund, N. Pogaku, M. Prodanovic, C. Hernandez-Aramburo, T.C. Green, "Energy management in autonomous microgrid using stability-constrained droop control of inverters," *IEEE Trans. Power Electron*., vol.23, no.5, pp.2346-2352, Sept. 2008.

[31] G. Diaz, C. Gonzales-Moran, J. Gomez-Aleixandre, and A. Diez, "Complex-valued state matrices for simple representation of large autonomous microgrids suppled by PQ and Vf generation," *IEEE Trans. Power Syst.*, vol. 24, no. 4, pp. 1720-1730, Nov. 2009.

[32] S. V. Iyer, M. N. Belur, and M. C. Chandorkar, "A generalized computational method to determine stability of a multi-inverter microgrid," *IEEE Trans. Power Electron.*, vol. 25, no.9, pp. 2420-2432, Sept. 2010.

[33] P. Mattavelli, A. M. Stankovic, and George C. Verghese, "SSR analysis with dynamic phasor model of thyristor-controlled series capacitor," *IEEE Trans. Power Syst.*, vol. 14, no. 1, pp. 200-208, Feb. 1999.

[34] H. Ruiwen, and C. Zexiang, "Modeling and harmonic analysis of TCSC with dynamic phasors," *in: Proc. IEEE/PES Transmission and Distribution Conference & Exhibition*, pp. 1–5, 2005

[35] P.C. Stefanov, and A.M. Stankovic, "Modeling of UPFC operation udder unbalanced conditions with dynamic phasors," *IEEE Trans. Power Syst.*, vol. 17, no. 2, pp. 395–403, May 2002.

[36] E. Zhijun , K. Chan, and D. Fang, "Dynamic phasor modelling of TCR based FACTS devices for high speed power system fast transients simulation," *Asian Power Electronics Journal*, vol. 1, no. 1, pp. 42-48, Aug. 2007.

[37] E. A. A. Coelho, P. C. Cortizo, and P. F. D. Garcia, "Small signal stability for single phase inverter connected to stiff AC system," *in Conf. Rec. 34th IEEE IAS Annu. Meeting*, Oct. 3–7, 1999, vol. 4, pp. 2180–2187.

[38] E. A. A. Coelho, P. C. Cortizo, and P. F. D. Garcia, "Small signal stability for parallel-connected inverters in standalone AC supply systems," *IEEE Trans. Ind. Appl.*, vol. 38, no. 2, pp. 533–542, Mar./Apr. 2002.

[39] S. R. Sanders, J. M. Noworolski, X. Liu, and G. C. Verghese, "Generalized averaging method for power conversion circuits ,"*IEEE Trans. Power Electron.*, vol. 6, no.2, pp. 251-259, Apr. 1991.

[40] D. Maksimovic, A. M. Stankovic, V. J. Thottuvelil, and G. C. Verghese, "Modeling and simulation of power electronic converters," *Proceedings of The IEEE*, vol. 89, no.6, pp. 898-912, Jun. 2001.